

# A Novel Single-Phase Bidirectional Nine-Level Converter Employing Four Quadrant Switches

Vitor Monteiro

Industrial Electronics Department  
ALGORITMI Research Centre  
University of Minho  
Guimarães – Portugal  
vmonteiro@dei.uminho.pt

Tiago J. C. Sousa

Industrial Electronics Department  
ALGORITMI Research Centre  
University of Minho  
Guimarães – Portugal  
tsousa@dei.uminho.pt

Carlos Couto

Industrial Electronics Department  
ALGORITMI Research Centre  
University of Minho  
Guimarães – Portugal  
ccouto@dei.uminho.pt

M. J. Sepúlveda

Industrial Electronics Department  
ALGORITMI Research Centre  
University of Minho  
Guimarães – Portugal  
mjs@dei.uminho.pt

J. C. Aparício Fernandes

Industrial Electronics Department  
ALGORITMI Research Centre  
University of Minho  
Guimarães – Portugal  
aparicio@dei.uminho.pt

João L. Afonso

Industrial Electronics Department  
ALGORITMI Research Centre  
University of Minho  
Guimarães – Portugal  
jla@dei.uminho.pt

**Abstract**—A novel bidirectional ac-dc multilevel converter based on four quadrant switches is proposed. This new converter can establish nine voltage levels downstream the coupling filter used to interface with the power grid, and, comparing with conventional two- or three-level converters, it operates with improved ac-side current, both for operation as active rectifier (on-grid), grid-tied inverter (on-grid) or voltage inverter (off-grid). A detailed description of the converter is exhibited, highlighting its main advantages according to the applications where it can be employed in smart grid scenarios. In order to confirm its viability, a considerable set of results is presented and discussed, establishing an overall comparison with conventional converters. Moreover, the proposed converter is validated operating as active rectifier, as grid-tied inverter, and as voltage inverter, controlled in closed-loop by current or voltage. The details of the proposed power converter hardware and the implementation of the digital algorithm, based on a fixed switching frequency structure, are clarified and discussed throughout the paper.

**Keywords**—Multilevel Converter; Nine-Level Converter; Four Quadrant Switches; Digital Control, Power Quality.

## I. INTRODUCTION

Active rectifiers or power factor correction (PFC) topologies offer a dominant solution in the industrial electronics sector to prevent power quality problems in single- and three-phase interfaces [1][2][3]. A high power factor and a reduced harmonic distortion in the ac-side current are notorious advantages in counterpart of the usual passive rectifiers [4][5][6]. A complete assessment of converters for active rectifiers is offered in [3], highlighting unidirectional and bidirectional interfaces, buck- and boost-type structures, multilevel characteristics and interleaved arrangements, as well as operation in isolated mode. Similar studies can be found specifically for bridgeless structures [7][8], Vienna-type topologies [9], and cascade converters [10][11]. Considering all of these characteristics, multilevel converters have a special interest, since an improved ac-side current can be achieved increasing the voltage levels, which are resultant from the association of power devices and voltage sources [12][13].

The essential circuits and control schemes for multilevel configurations are presented in [14] and [15], analysis of multilevel configurations for different industrial purposes are presented in [15] and [16], a review of multilevel converters

with reduced number of power devices is presented in [17], and comprehensive reviews of modular multilevel converters are presented in [18] and [19]. Besides a high power factor and a reduced harmonic distortion in the ac-side current, reduced power losses and voltage stress in the switching devices can be achieved by employing topologies based on multilevel converters. Since the number of voltage levels is directly proportional to the required hardware (e.g., voltage sensors), usually, the number of distinct voltage levels is limited for industrial applications. Examples of multilevel converters proposed in literature include a five-level Vienna rectifier for electric vehicle battery chargers [20], a nine-level topology based on a neutral point clamped structure for motor drivers [21], a cascade multilevel structure based on the series connection of H-bridge units [22], a multilevel converter for a universal series-parallel conditioner [23], a five-level flying capacitor topology for motor drivers [24], a nine-level cascaded-transformer converter for grid-tied applications [25], a seven-level active rectifier constituted by asymmetrical H-bridge cells [26], a five-level diode-clamped arrangement for ac-ac converters [27], a cascade multilevel employing a single dc-source [28], a single-stage multilevel converter with a full-bridge-based structure [29], and a five-level H-bridge configuration for active conditioners [30].

In the context of multilevel converters, a single-phase bidirectional nine-level converter is proposed in this paper. The circuit topology is presented in Fig. 1 for a grid interface, i.e., allowing an operation as active rectifier or grid-tied inverter. A similar multilevel converter is proposed in [31], but for five voltage levels and where a four-quadrant switch is employed based on four diodes and a switching device. An improved topology based on two diodes and two switching devices is proposed in [32] for unidirectional and in [33] for bidirectional systems, but both for five-levels. In this follow-up, a seven-level converter is proposed in [34] also employing four-quadrant switches based on four diodes and a switching device. A nine-level converter is proposed in [35], but also employing four-quadrant switches based on four diodes and a switching device. In all of these cases, the current flows by two diodes and by a switching device, i.e., the double of diodes and switching devices are required when comparing with the proposed converter in this paper. A nine-level converter based on stacked multilevel concepts is proposed in

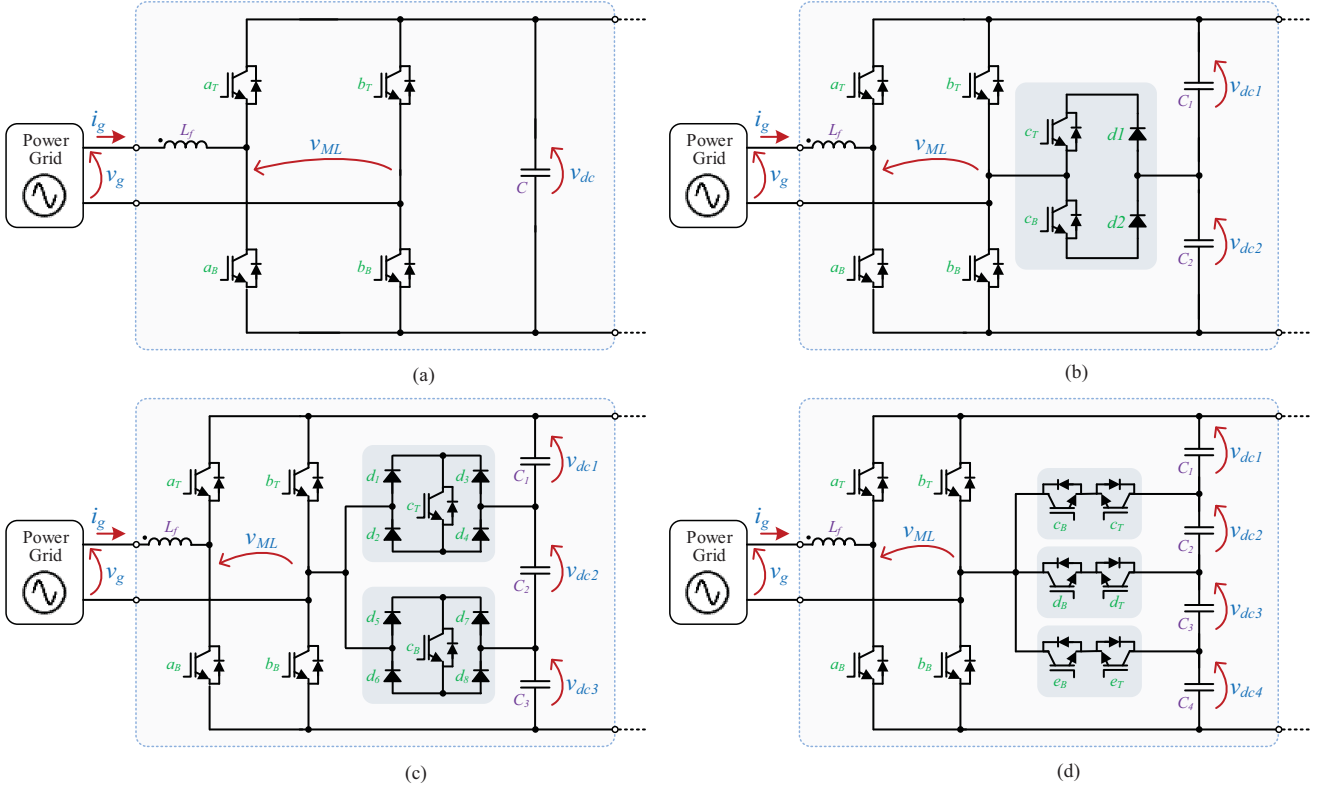


Fig. 1. Multi-level bidirectional topologies for applications of active rectifiers or grid-tied inverters: (a) Three-level full-bridge; (b) Five-level full-bridge; (c) Seven-level full-bridge; (d) Proposed nine-level full-bridge.

[36], but it requires a complex structure of cascade stacked flying capacitors and coupled inductors. A nine-level converter based on a cascade H-bridge is proposed in [37], but it requires a low-voltage and a high-voltage h-bridge with a single dc-source. Summarizing, this paper proposes a nine-level converter with reduced number and optimized utilization of switching devices, and with the possibility to operate in bidirectional mode, which is an interesting feature for industrial applications, e.g., for back-to-back structures, electric vehicle battery chargers for smart grids, and indirect ac-to-ac converters.

The paper is organized as follows: Section II exhibits the nine-level converter, establishing a comparison with conventional three-, five-, and seven-level converters; Section III introduces the control algorithm based on a fixed switching frequency; Section IV presents and discusses the obtained results; Section V closes the paper with the conclusions.

## II. THEORETICAL ANALYSIS: STRUCTURE OF THE NINE-LEVEL CONVERTER

Fig. 1 shows the evolution from the classical bidirectional three-level full-bridge converter to the proposed nine-level converter, passing from five- and seven-level structures. Among the large variety of state-of-the-art multilevel converters, the presented ones were selected aiming to establish a parallelism with the proposed converter, both in terms of front-end structure (H-bridge) and split dc-link. The converter presented in Fig. 1(a) is the simplest in terms of hardware and control algorithm, however, it is a three-level converter requiring an appropriate arrangement for the coupling passive filters in order to eliminate the high-frequency switching harmonics. In this converter, at least, each switching device should be selected for a voltage  $v_{dc}$  and a current  $i_g$ . Aiming to improve the ac-side current and to reduce the arrangement for the coupling passive filters, an

improved five-level converter is presented in Fig. 1(b) [32], employing a single four-quadrant switch composed by two diodes and two switching devices. In this converter, the switching devices  $a_T$  and  $a_B$  of the full-bridge should be selected for a voltage  $v_{dc}$  and a current  $i_g$ , and the remaining switching devices and diodes for a voltage  $v_{dc}/2$  and a current  $i_g$ . Applying the same reasoning of a split dc-link, a seven-level converter is presented in Fig. 1(c) [34], employing two four-quadrant switches, each one composed by four diodes and a switching device. The maximum voltages and currents for each switching devices and diode is very similar to the previous case. Deriving from the previous topologies, the proposed converter is presented in Fig. 1(d). As shown, it is constituted by three four-quadrant switches, each one composed by two switching devices. In this converter, the switching devices of the full-bridge should be selected for a voltage  $v_{dc}$  and a current  $i_g$ , the four-quadrant switches formed by  $c_T$ - $c_B$  and  $e_T$ - $e_B$  for a voltage  $3v_{dc}/4$ , the four-quadrant switch formed by  $d_T$ - $d_B$  for a voltage  $v_{dc}/2$ , all for a current  $i_g$ .

Considering as example the three-level converter presented in Fig. 1(a), and using an inductor as coupling filter, the required value of inductance is determined as function of the current ripple ( $\Delta i_g$ ), switching frequency ( $f_s$ ) and dc-link voltage ( $v_{dc}$ ) voltage as:

$$L = \frac{v_{dc}}{4\Delta i_g f_s}. \quad (1)$$

Comparing with the nine-level converter (cf. Fig. 1(d)), and considering the same value of inductance the current ripple is reduced for  $\Delta i_g/4$ . Therefore, if it intended to maintain the same value of  $\Delta i_g$ , then the inductance value can be reduced 25% comparing with the classical approach. The functional voltage levels of the bidirectional nine-level converter are presented in Fig. 2. As presented in Table I, the voltage levels are designated according to the state

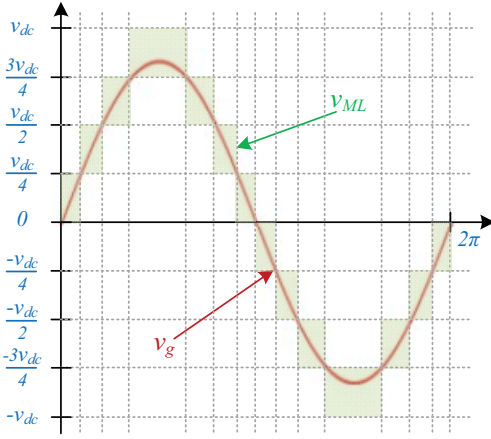


Fig. 2. Operating voltage levels of the proposed bidirectional nine-level converter according to the grid voltage ( $v_g$ ).

TABLE I  
STATE OF EACH IGBT FOR PRODUCING THE NINE VOLTAGE LEVELS

	$a_T$	$a_B$	$b_T$	$b_B$	$c_T$	$c_B$	$d_T$	$d_B$	$e_T$	$e_B$	$v_{ML}$
$v_g > 0$	ON	OFF	OFF	ON	OFF	OFF	OFF	OFF	OFF	OFF	$v_{dc}$
	ON	OFF	OFF	OFF	OFF	OFF	OFF	OFF	ON	ON	$3v_{dc}/4$
	ON	OFF	OFF	OFF	OFF	OFF	ON	ON	OFF	OFF	$v_{dc}/2$
	ON	OFF	OFF	OFF	ON	ON	OFF	OFF	OFF	OFF	$v_{dc}/4$
	ON	OFF	ON	OFF	OFF	OFF	OFF	OFF	OFF	OFF	0
$v_g < 0$	OFF	ON	OFF	ON	OFF	OFF	OFF	OFF	OFF	OFF	0
	OFF	ON	OFF	OFF	OFF	OFF	OFF	OFF	ON	ON	$-v_{dc}/4$
	OFF	ON	OFF	OFF	OFF	OFF	ON	ON	OFF	OFF	$-v_{dc}/2$
	OFF	ON	OFF	OFF	ON	ON	OFF	OFF	OFF	OFF	$-3v_{dc}/4$
	OFF	ON	ON	OFF	OFF	OFF	OFF	OFF	OFF	OFF	$-v_{dc}$

of each switching device, in this case IGBTs. The IGBTs  $a_T$ ,  $a_B$ ,  $b_T$  and  $b_B$  are switched at the grid voltage frequency (supporting a maximum voltage of  $v_{dc}$ ) and the remaining IGBTs are switched at high frequency (i.e., at the switching frequency) to obtain the voltage levels  $v_{dc}/4$ ,  $v_{dc}/2$ ,  $3v_{dc}/4$ ,  $v_{dc}$ ,  $-v_{dc}/4$ ,  $-v_{dc}/2$ ,  $-3v_{dc}/4$ , and  $-v_{dc}$ . The maximum voltage across the IGBTs  $c_T$ - $c_B$  and  $e_T$ - $e_B$  is  $3v_{dc}/4$  and the maximum voltage across the IGBTs  $d_T$ - $d_B$  is  $v_{dc}/2$ . Therefore, it is possible to optimize the switching losses of these IGBTs facing the other ones.

This is valid for both for active rectifier (on-grid), grid-tied inverter (on-grid) or voltage inverter operation (off-grid). The illustrations of the IGBTs switching sequences are presented in Fig. 3. These switching sequences, which are in accordance with Table I, are presented for the positive (cf. Fig. 3(a-e)) and for the negative (Fig. 3(f-j)) half-cycles. In the positive half-cycle, the IGBT  $a_T$  is always ON and the IGBT  $a_B$  is always OFF, and in the negative half-cycle the IGBT  $a_B$  is ON and the IGBT  $a_T$  is OFF. The dc-link voltage balancing is obtained selecting the proper state of the converter to charge or discharge each capacitor. It is imperative to note that for a bidirectional process, it is necessary to use all the switching devices (IGBTs), however, for a unidirectional operation, for instance, just for applications of active rectifiers, some IGBTs (e.g.,  $a_T$  and  $a_B$ ) can be substituted by diodes, maintaining the same principle of operation. Fig. 3 shows the pair of IGBTs used to form each four-quadrant switch (cf.  $c_T$ - $c_B$ ,  $d_T$ - $d_B$ , and  $e_T$ - $e_B$ ). These IGBTs are switched at the same time, however, a strategy to switch a single IGBT and use the reverse diode of the other IGBT can be adopted, resulting in a more complex control strategy and required hardware. Taking into account this reason, for the four-quadrant switches it was adopted the strategy of IGBTs with a common emitter configuration to

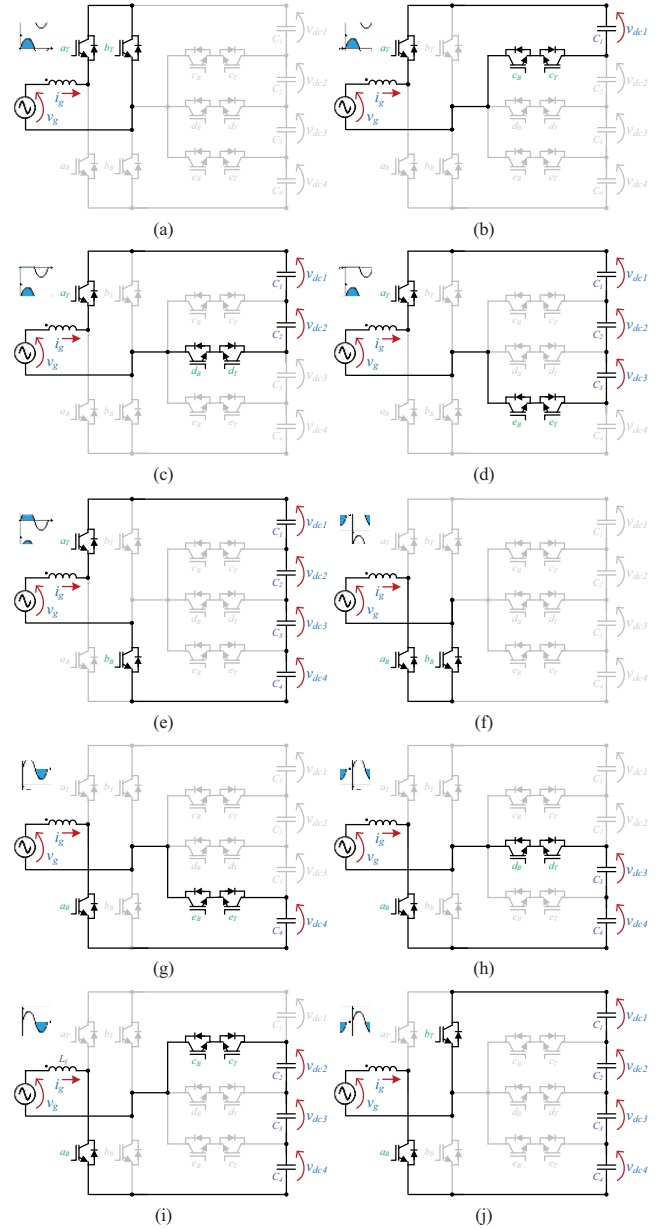


Fig. 3. Switching sequences of the states assumed by the bidirectional nine-level converter during the positive (a)-(e) and negative half-cycles (f)-(j).

facilitate the implementation of the IGBTs gate-drivers in both active rectifier (on-grid), grid-tied inverter (on-grid) or voltage inverter operation (off-grid) operation. Since the IGBTs  $a_T$ ,  $a_B$ ,  $b_T$ , and  $b_B$  are used to define the voltage levels  $+v_{dc}$ , 0 (with a redundant state), and  $-v_{dc}$ , the pairs of IGBTs  $c_T$ - $c_B$ ,  $d_T$ - $d_B$ , and  $e_T$ - $e_B$  are used to define the intermediary states  $3v_{dc}/4$ ,  $v_{dc}/2$ ,  $v_{dc}/4$ ,  $-v_{dc}/4$ ,  $-v_{dc}/2$ , and  $-3v_{dc}/4$ .

### III. DIGITAL CONTROL ALGORITHM BASED ON A FIXED SWITCHING FREQUENCY

With a digital control executed with a fixed sampling and switching frequency and a pulse-width modulation (PWM) strategy based on a single unipolar carrier, it was indispensable to implement a scheme to modify the reference voltage defined by the current or voltage control strategy (cf. section II). The scheme used to modify the reference ( $v_{ML}^*$ ) used to compare with the PWM carrier is presented in Fig. 4. The reference voltages  $v_{ML1}^*$  and  $v_{ML2}^*$  are obtained from the original signal  $v_{ML}^*$ , where, the sum of  $v_{ML1}^*$  with  $v_{ML2}^*$  results in  $v_{ML}^*$ . Throughout the positive half-cycle, the



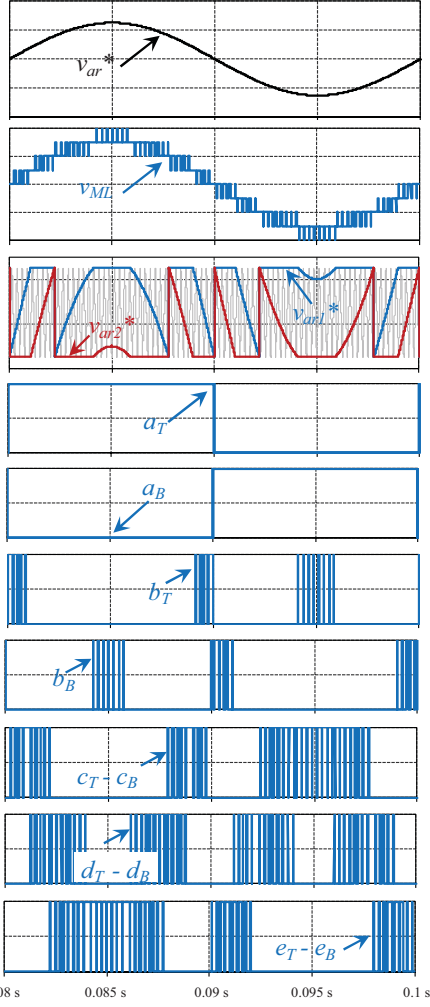


Fig. 4. Scheme used to modify the reference voltage defined by the current or voltage control in order to obtain the IGBTs gate-pulse patterns for the nine-level converter.

```

227 if( vML>0 ) {
228     //0 to vdc/4
229     if( vML<=amp ) { vML1=vML; vML2=0; }
230     //vdc/4 to vdc/2
231     if( vML>amp ) { vML1=amp; vML2=vML-amp; }
232     //vdc/2 to 3vdc/4
233     if( vML>=2.0*amp ) { vML1=vML-2.0*amp; vML2=0; }
234     //3vdc/4 to vdc
235     if( vML>=3.0*amp ) { vML1=amp; vML2=(vML-3.0*amp); }
236 }
237
238 else{
239     //0 to vdc/4
240     if( vML>=-amp ) { vML1=amp; vML2=(vML+1*amp); }
241     //-vdc/4 to -vdc/2
242     if( vML<=-amp ) { vML1=(vML+2*amp); vML2=0; }
243     //-vdc/2 to -3vdc/4
244     if( vML<=-2.0*amp ) { vML1=amp; vML2=(vML+1*amp); }
245     //-3vdc/4 to -vdc
246     if( vML<=-3.0*amp ) { vML1=(vML+4*amp); vML2=0; }
247 }

```

Fig. 5. Digital code implementation for obtaining the modified reference voltages  $v_{ML1}^*$  and  $v_{ML2}^*$  from  $v_{ML}^*$ .

reference  $v_{ML1}^*$  is compared with the carrier to define the voltage levels 0,  $+v_{dc}/4$ ,  $+v_{dc}/2$ , and  $+3v_{dc}/4$ , and throughout the negative half-cycle to define the voltage levels  $-v_{dc}/4$ ,  $-v_{dc}/2$ ,  $-3v_{dc}/4$  and  $-v_{dc}$ . Throughout the positive half-cycle, the reference  $v_{ML2}^*$  is compared with the carrier to define the voltage levels  $+v_{dc}/4$ ,  $+v_{dc}/2$ ,  $+3v_{dc}/4$  and  $+v_{dc}$ , and throughout the negative half-cycle to define the voltage levels 0,  $-v_{dc}/4$ ,  $-v_{dc}/2$ , and  $-3v_{dc}/4$ . Fig. 5 presents the digital code implementation for obtaining the modified reference voltages  $v_{ML1}^*$  and  $v_{ML2}^*$  from  $v_{ML}^*$ . The variable *amp* means the maximum amplitude of the unipolar PWM carrier. By using the resultant signals from the comparison between the

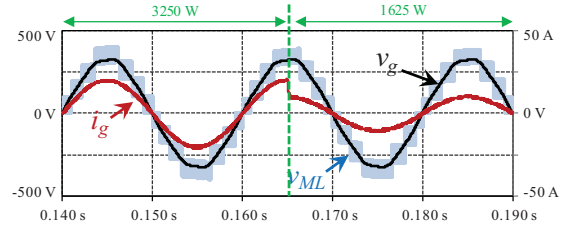


Fig. 6. Operation of the nine-level converter as active rectifier controlled by current: Grid voltage ( $v_g$ ); Ac-side current ( $i_g$ ); Voltage levels ( $v_{ML}$ ).

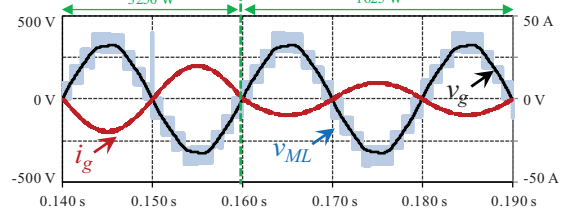


Fig. 7. Operation of the nine-level converter as grid-tied inverter controlled by current: Grid voltage ( $v_g$ ); Ac-side current ( $i_g$ ); Voltage levels ( $v_{ML}$ ).

reference voltages  $v_{ML1}^*$  and  $v_{ML2}^*$  with the PWM carrier, a combinational logic for enable/disable is applied for obtaining the control signals for the all the IGBTs. During the operation with current control feedback, the control law applied to attain the reference voltage  $v_{ML}^*$  is based on the converter analysis in the grid-side, where the reference voltage ( $v_{ML}^*$ ) during a sampling period ( $T_s$ ) is achieved as:

$$v_{ML}^*[k] = T_s^{-1} L_f i_g[k] + v_g[k] - T_s^{-1} L_f i_g^*[k], \quad (2)$$

where the reference current is determined by:

$$i_g^*[n] = \sqrt{2} \frac{p_{dc}[n]}{V_G[n]} \sin[\phi]. \quad (3)$$

with  $p_{dc}$  defined by the operating power and  $V_G$  by the rms value of the grid voltage. During the operation with voltage control feedback, the control law applied to attain the reference voltage  $v_{ML}^*$  is achieved as:

$$v_{ML}^*[k] = T_s^{-1} L_f i_g[k] + v_g^*[k] - T_s^{-1} L_f i_g[k-1], \quad (4)$$

with  $v_g^*$  determined by the required voltage of the connected load. The reference voltage  $v_g^*$  is determined according to the application. For instance, in motor driver applications, the reference voltage is adjusted according to the control algorithms and in uninterruptible power supplies (UPSs) the reference voltage is determined by the rms value of the grid voltage. It is important to highlight that the nine-level converter can be controlled by other current or voltage strategies maintaining the same modulation. For instance, proportional-integral, sliding mode, or predictive strategies can be applied in the feedback control maintaining the same features of the nine-level converter.

#### IV. ANALYSIS AND SIMULATION

The validation was considered during the operation as active rectifier (on-grid), grid-tied inverter (on-grid) or voltage inverter operation (off-grid). Fig. 6 and Fig. 7 shows the obtained results during the operation as active rectifier (on-grid) and grid-tied inverter (on-grid). A simulation model was developed in PSIM for a rms nominal grid voltage of 230 V, a dc-link voltage of 400 V, and a maximum active power of 3.5 kW. For the grid coupling filter, it was selected an inductor with nominal value of 1 mH, and four capacitors with a total capacitance of 3 mF for the dc-link. The design of the passive filters, as well as the assessment of the voltage and current control feedback in steady- and transient-state are out

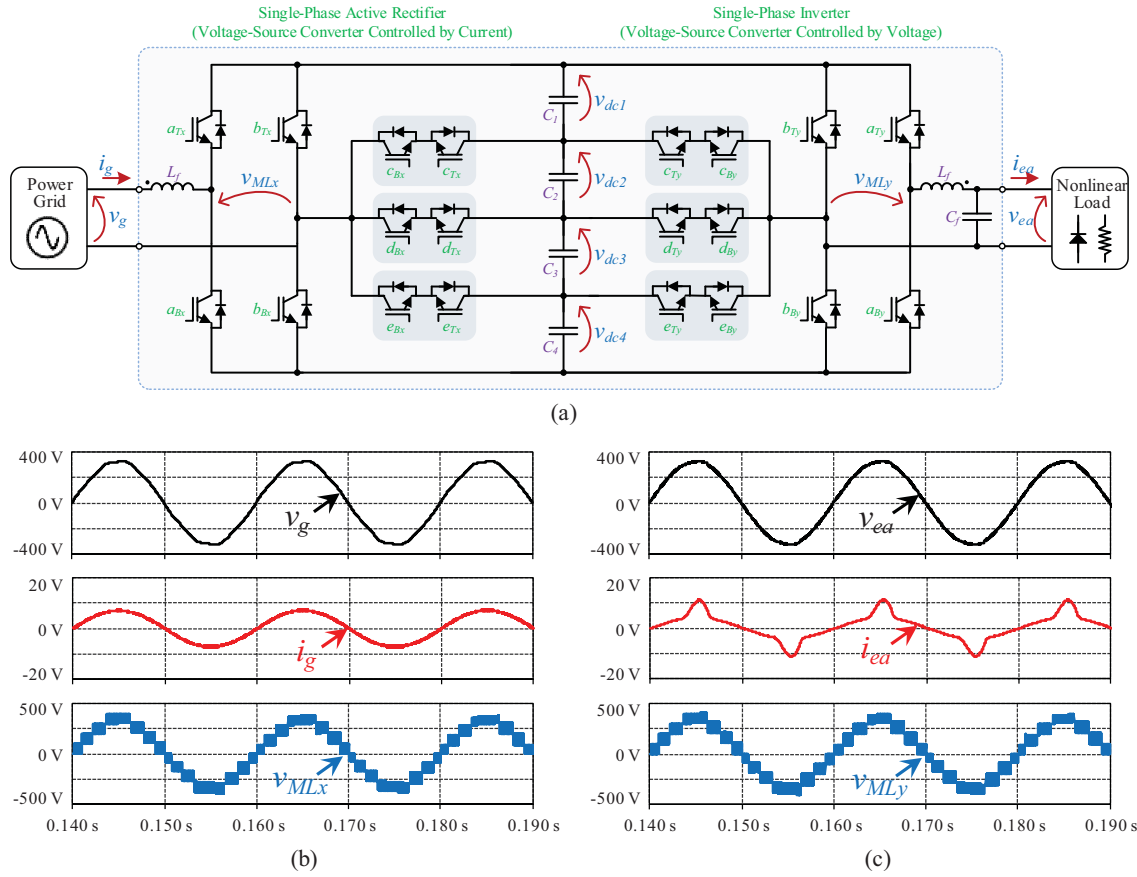


Fig. 8. Two of the proposed nine-level converter in back-to-back configuration: (a) Topology; (b) Results of the active rectifier operation; (c) Results of the voltage-inverter operation.

of the scope of this paper, since, several strategies with advantages/disadvantages can be adopted for numerous purposes. The operation as active rectifier was validated, since the converter can be adopted in different applications, e.g., for electric vehicle battery chargers and power factor correction topologies. As active rectifier, the nine-level converter operates as a voltage-source converter controlled by current, i.e., the grid imposes the voltage and the ac-side current is controlled according to the operating power of the application. Fig. 6 shows the results during this mode considering an operating power with a sudden variation of 50% from about 3.3 kW to 1.6 kW. As it can be observed, the ac-side current ( $i_g$ ) is sinusoidal and in phase with the grid voltage ( $v_g$ ), and the nine-levels are established in the output voltage of the converter ( $v_{ML}$ ). The operation as grid-tied inverter was also validated, since the converter can be used for different applications, e.g., as inverter for renewables. Also in this case, the nine-level converter operates as a voltage-source converter controlled by current, but injecting a current into the power grid, since the grid imposes the voltage. Fig. 7 shows the results in this mode considering an operating power with a sudden variation of 50% from about 3.3 kW to 1.6 kW. In this case, the nine voltage levels ( $v_{ML}$ ) are established and the ac-side current ( $i_g$ ) is also sinusoidal, but in phase opposition with the voltage. The nine-level converter was also validated considering a back-to-back configuration, where a converter operates in active rectifier mode and the other in inverter mode (e.g., for applications of on-line UPSs, voltage inverters of isolated systems, or for motor drivers). Therefore, it was possible to validate the nine-level converter operating as a voltage-source converter controlled by voltage. In this case, besides the aforementioned values for the grid side in terms of voltage and current, a rms voltage of 230 V and an apparent

power of 1.2 kVA were considered. In the electrical appliances side, it was selected an LC filter with an inductor of 1 mH and a capacitor of 5  $\mu$ F. Fig. 8(a) shows the back-to-back configuration employing two nine-level converter, sharing the same dc-link. Aiming to consider a real scenario of application, one of the converters was connected to the power grid (controlled by current) and the other to a set of nonlinear electrical appliances (controlled by voltage). In this scenario, the nine-level converter imposes a sinusoidal voltage even with a current with a high-level of harmonic distortion. Fig. 8(b) and Fig. 8(c) show the obtained results for ac voltages ( $v_g$  and  $v_{ea}$ ), ac currents ( $i_g$  and  $i_{ea}$ ), and voltage levels ( $v_{MLx}$  and  $v_{MLy}$ ) for both operating modes. In the grid side, the voltage ( $v_g$ ) has a THD of 1.9% and the current ( $i_g$ ) a THD of 0.9%. In the electrical appliance side, the voltage ( $v_{ea}$ ) has a THD of 1.1% and the current ( $i_{ea}$ ) a THD of 79.2%.

## V. CONCLUSIONS

A single-phase bidirectional nine-level full-bridge converter, based on four quadrant switches and a split dc link, is proposed as a contribution to improve power quality issues. A comprehensive explanation of the digital implementation is presented and discussed throughout the paper. By selecting the precise distinct switching sequences, the multilevel converter has the ability to state nine voltage levels throughout the positive and negative half cycles. The validation was conducted considering the nine-level converter operating as active rectifier (on-grid), as grid-tied inverter (on-grid) and as voltage inverter operation (off-grid) controlled in closed-loop by current or voltage. The obtained results show the advantages and viability of the proposed converter for a wide range of industrial applications in smart grid scenarios.

## ACKNOWLEDGMENT

This work has been supported by COMPETE: POCI-01-0145-FEDER-007043 and FCT – Fundação para a Ciência e Tecnologia within the Project Scope: UID/CEC/00319/2013. This work is financed by the ERDF – European Regional Development Fund through the Operational Programme for Competitiveness and Internationalisation – COMPETE 2020 Programme, and by National Funds through the Portuguese funding agency FCT within project SAICTPAC/0004/2015 – POCI – 01-0145-FEDER-016434. Mr. Tiago Sousa is supported by the doctoral scholarship SFRH/BD/134353/2017 granted by of the FCT project 0302836 NORTE-01-0145-FEDER-030283.

## REFERENCES

- [1] Johann W. Kolar, Thomas Friedli, "The Essence of Three-Phase PFC Rectifier Systems—Part I," *IEEE Trans. Power Electron.*, vol.28, no.1, pp.176-198, Jan. 2013.
- [2] Thomas Friedli, Michael Hartmann, Johann W. Kolar, "The Essence of Three-Phase PFC Rectifier Systems—Part II," *IEEE Trans. Power Electron.*, vol.29, no.2, pp.543-560, Feb. 2014.
- [3] Bhim Singh, Brij N. Singh, Ambrish Chandra, Kamal Al-Haddad, Ashish Pandey, Dwarka P. Kothari, "A Review of Single-Phase Improved Power Quality AC-DC Converters," *IEEE Trans. Ind. Electron.*, vol.50, no.5, pp.962-981, Oct. 2003.
- [4] Oscar García, José A. Cobos, Roberto Pietro, Pedro Alou, Javier Uceda, "Single Phase Power Factor Correction: A Survey," *IEEE Trans. Power Electron.*, vol.18, no.3, pp.749-755, May 2003.
- [5] Fernando Beltrame, Leandro Roggia, Luciano Schuch, José Renes Pinheiro, "A Comparison of High Power Single-Phase Power Factor Correction Pre-Regulators," *IEEE ICIT Industrial Technology*, pp.625-630, Mar. 2010.
- [6] Huai Wei, Issa Batarseh, "Comparison of Basic Converter Topologies for Power Factor Correction," *IEEE Proceedings of Southeastcon*, pp.348-353, Apr. 1998.
- [7] André De Bastiani Lange, Thiago Batista Soeiro, Márcio Silveira Ortmann, Marcelo Lobo Heldwein, "Three-Level Single-Phase Bridgeless PFC Rectifiers," *IEEE Trans. Power Electron.*, vol.30, no.6, pp.2935-2949, June 2015.
- [8] Laszlo Huber, Yungtaek Jang, Milan Jovanovic, "Performance Evaluation of Bridgeless PFC Boost Rectifier," *IEEE Trans. Power Electron.*, vol.23, no.3, pp.1381-1390, May 2008.
- [9] Hani Vahedi, Philippe-Alexandre Labbé, Kamal Al-Haddad, "Single-Phase Single-Switch Vienna Rectifier as Electric Vehicle PFC Battery Charger," *IEEE VPPC Vehicle Power and Propulsion Conference*, pp.1-6, Oct. 2015.
- [10] Mariusz Malinowski, K. Gopakumar, Jose Rodriguez, Marcelo A. Perez, "A Survey on Cascaded Multilevel Inverters," *IEEE Trans. Ind. Electron.*, vol.57, no.7, pp.2197-2206, July 2010.
- [11] Ebrahim Babaei, Sara Laali, Somayeh Alilu, "Cascaded Multilevel Inverter with Series Connection of Novel H-Bridge Basic Units," *IEEE Trans. Ind. Electron.*, vol.31, no.12, pp.6664-6671, Dec. 2014.
- [12] Rasoul Shalchi Alishah, Daryoosh Nazarpour, Seyed Hossei Hosseini, Mehran Sabahi, "Novel Topologies for Symmetric, Asymmetric, and Cascade Switched-Diode Multilevel Converter With Minimum Number of Power Electronic Components," *IEEE Trans. Ind. Electron.*, vol.61, no.10, pp.5300-5310, Oct. 2014.
- [13] A. Pandey, B. Singh, B. N. Singh, A. Chandra, K. Al-Haddad, D. P. Kothari, "A Review of Multilevel Power Converters," *Journal of the Institution of Engineers*, vol.8, pp.220-231, Mar.2006.
- [14] Hirofumi Akagi, "Multilevel Converters: Fundamental Circuits and Systems," *Proc. IEEE*, vol.105, no.11, pp.2048-2065, Apr. 2017.
- [15] José Rodríguez, Jih-Sheng Lai, Fang Zheng Peng, "Multilevel Inverters: A Survey of Topologies, Controls, and Applications," *IEEE Trans. Ind. Electron.*, vol.49, no.4, pp.724-738, Aug. 2002.
- [16] Jih-Sheng Lai, Fang Zheng Peng, "Multilevel Converters-A New Breed of Power Converters," *IEEE Trans. Ind. Appl.*, vol.32, no.3, pp.509-517, May 1996.
- [17] Krishna Kumar Gupta, Alekh Ranjan, Pallavee Bhatnagar, Lalit Kumar Sahu, Shailendra Jain, "Multilevel Inverter Topologies With Reduced Device Count: A Review," *IEEE Trans. Power Electron.*, vol.31, no.1, pp.135-151, Jan. 2016.
- [18] Suman Debnath, Jiangchao Qin, Behrooz Bahrani, Maryam Saediard, Peter Barbosa, "Operation, Control, and Applications of the Modular Multilevel Converter: A Review," *IEEE Trans. Power Electron.*, vol.30, no.1, pp.37-53, Jan. 2015.
- [19] Alireza Nami, Jiaqi Liang, Frans Dijkhuizen, Georgios D. Demetriades, "Modular Multilevel Converters for HVDC Applications: Review on Converter Cells and Functionalities," *IEEE Trans. Power Electron.*, vol.30, no.1, pp.18-36, Jan. 2015.
- [20] Vítor Monteiro, Andrés A. Nogueiras Meléndez, João L. Afonso, "Novel Single-Phase Five-Level VIENNA-Type Rectifier with Model Predictive Current Control," *IEEE IECON Industrial Electronics Conference*, pp.6413-6418, Nov. 2017.
- [21] Teenu Techela Davis, Anubrata Dey, "Nine Level T-type Neutral Point Clamped Voltage Source Inverter for Induction Motor Drive," *IEEE IECON Industrial Electronics Conference*, pp.1331-1336, Nov. 2017.
- [22] Ebrahim Babaei, Sara Laali, Somayeh Alilu, "Cascaded Multilevel Inverter with Series Connection of Novel H-Bridge Basic Units," *IEEE Trans. Ind. Electron.*, vol.31, no.12, pp.6664-6671, Dec. 2014.
- [23] Leon M. Tolbert, Fang Z. Peng, Thomas G. Habetler, "A Multilevel Converter-Based Universal Power Conditioner," *IEEE Trans. Ind. Appl.*, vol.36, no.2, pp.596-603, Mar. 2000.
- [24] P. Roshankumar, P. P. Rajeevan, K. Mathew, K. Gopakumar, Jose I. Leon, Leopoldo G. Franquelo, "A Five-Level Inverter Topology with Single-DC Supply by Cascading a Flying Capacitor Inverter and an H-Bridge," *IEEE Trans. Power Electron.*, vol.27, no.8, pp.3505-3512, Aug. 2012.
- [25] Hossein Khoun Jahan, Kazem Zare, and Mehdi Abapour, "Verification of a Low Component Nine-Level Cascaded-Transformer Multilevel Inverter in Grid-Tied Mode," *IEEE J. Emerg. Sel. Topics Power Electron.*, vol.6, no.1, pp.429-440, Mar. 2018.
- [26] Jiangang Han, Tianhao Tang, "A Multilevel Active Rectifier Based on Series Connection of Asymmetrical H-Bridge Cells," *PRZEGLĄD ELEKTROTECHNICZNY*, pp.88-91, no.3, 2013.
- [27] Gabriel H. P. Ooi, Ali I. Maswood, Ziyu Lim, "Five-Level Multiple-Pole PWM AC-AC Converters With Reduced Components Count," *IEEE Trans. Ind. Electron.*, vol.62, no.8, pp.4739-4748, Aug. 2015.
- [28] Zhong Du, Leon M. Tolbert, John N. Chiasson, Burak Özpıneci, "A Cascade Multilevel Inverter Using a Single DC Source," *IEEE APEC Applied Power Electronics Conference and Exposition*, pp.426-430, Mar. 2006.
- [29] Mehdi Narimani, Gerry Moschopoulos, "A Novel Single-Stage Multilevel Type Full-Bridge Converter," *IEEE Trans. Ind. Electron.*, vol.60, no.1, pp.31-42, Jan. 2013.
- [30] Ahmed M. Massoud, Stephen J. Finney, Andrew J. Cruden, Barry W. Williams, "Three-Phase, Three-Wire, Five-Level Cascaded Shunt Active Filter for Power Conditioning, Using Two Different Space Vector Modulation Techniques," *IEEE Trans. Power Del.*, vol.22, no.4, pp.2349-2361, Oct. 2007.
- [31] Sung-Jun Park, Feel-Soon Kang, Man Hyung Lee, Cheul-U Kim, "A New Single-Phase Five-Level PWM Inverter Employing a Deadbeat Control Scheme," *IEEE Trans. Power Electron.*, vol.18, no.3, pp.831-843, May 2003.
- [32] Vítor Monteiro, João C. Ferreira, Andrés A. Nogueiras Meléndez, João L. Afonso, "Model Predictive Control Applied to an Improved Five-Level Bidirectional Converter," *IEEE Trans. Ind. Electron.*, vol.63, no.9, pp.5879-5890, Sept. 2016.
- [33] Vítor Monteiro, Andrés A. Nogueiras Meléndez, João C. Ferreira, Carlos Couto, João L. Afonso, "Experimental Validation of a Proposed Single-Phase Five-Level Active Rectifier Operating with Model Predictive Current Control," *IEEE IECON Industrial Electronics Conference*, pp.3939-3944, Nov. 2015.
- [34] Nasrudin A. Rahim, Krismadinata Chaniago, Jeyraj Selvaraj, "Single-Phase Seven-Level Grid-Connected Inverter for Photovoltaic System," *IEEE Trans. Ind. Electron.*, vol.58, no.6, pp.2435-2443, June 2011.
- [35] Gerardo Ceglia, Víctor Guzmán, Carlos Sánchez, Fernando Ibáñez, Julio Walter, María I. Giménez, "A New Simplified Multilevel Inverter Topology for DC-AC Conversion," *IEEE Trans. Power Electron.*, vol.21, no.5, pp.1311-1319, Sept. 2006.
- [36] Dan Florica, Dragos Ovidiu Kisck, "A New Nine-Level Boost PWM Rectifier Based on Stacked Multilevel Concepts," *IEEE IECON Industrial Electronics Conference*, pp.1077-1083, Dallas Texas USA, Oct. 2014.
- [37] Giampaolo Buticchi, Davide Barater, Emilio Lorenzani, Carlo Concar, Giovanni Franceschini, "A Nine-Level Grid-Connected Converter Topology for Single-Phase Transformerless PV Systems," *IEEE Trans. Ind. Electron.*, vol.61, no.8, pp.3951-3960, Aug. 2014.